

# Widespread hillslope gullying on the southeastern Tibetan Plateau: Human or climate-change induced?

Jon D. Pelletier<sup>1,†</sup>, Jay Quade<sup>1</sup>, Ron J. Goble<sup>2</sup>, and Mark S. Aldenderfer<sup>3,\*</sup>

<sup>1</sup>*Department of Geosciences, The University of Arizona, 1040 East Fourth Street, Tucson, Arizona 85721-0077, USA*

<sup>2</sup>*Department of Geosciences, University of Nebraska, 214 Bessey Hall, Lincoln, Nebraska 68588-0340, USA*

<sup>3</sup>*School of Anthropology, The University of Arizona, 1009 E. South Campus Drive, Tucson, Arizona 85721-0030, USA*

## ABSTRACT

Many drainage basins adjacent to the upper Tsangpo Valley on the southeastern Tibetan Plateau are pervasively gullied. These gullies expose a stratigraphic record alternating between slow aggradation and stability (i.e., soil development) for much of the Quaternary, suggesting that gullying is recent and unprecedented within at least the past 10–100 k.y. In this paper, we date the initiation of gullying at five sites in the region using optically stimulated luminescence (OSL). We also test alternative hypotheses for gully initiation using numerical landform evolution modeling. OSL ages constrain the initiation of gullying to be mid-to-late Holocene in age. This period coincides with the onset of pastoralism in the upper Tsangpo Valley. Numerical modeling suggests that a reduction in vegetation density during the colder, drier conditions of Pleistocene glacial intervals did not trigger gullying because the reduction in vegetation density and hence rates of colluvial deposition in valleys coincided with an unusually dry period less capable of significant fluvial erosion from valleys. As such, low-order valleys most likely did not incise prior to the mid-to-late Holocene because an approximate balance was maintained between colluvial deposition and fluvial erosion. Vegetation changes associated with the onset of pastoralism, however, may have triggered gullying because such changes lowered the rate of colluvial deposition in valleys and/or increased the rate of fluvial erosion in valleys. The results of this paper provide insight into the ways in which drainage basins respond to climatic and anthropogenic perturbations in semiarid climates of moderate

relief and underscore the dramatic landscape responses that can occur when geomorphic thresholds are crossed.

## INTRODUCTION

Gullies are vertical-walled channels that form in hillslopes and low-order fluvial valleys (Harvey et al., 1985). Gullies can form in response to base-level fall as incipient channels develop and/or deepen near the base level, triggering localization of overland/channel flow and incision in a positive feedback. Gullies can also form in the absence of base-level fall. Commonly, anthropogenic decreases in vegetation density are invoked as the dominant triggering mechanism for the development of such gullies (Valentin et al., 2005). For example, studies of gully initiation in Colorado (Graf, 1979), California (Farnsworth and Milliman, 2003), Michigan (Burkard and Kostaschuk, 1995), South Carolina (Galang et al., 2007), north-west England (Harvey, 1992), Spain (Garcia-Ruiz et al., 1997), New Zealand (Gomez et al., 2003; Marden et al., 2005), Australia (Prosser and Slade, 1994; Prosser and Soufi, 1998), and Madagascar (Wells and Andriamihaja, 1993) all attributed gully initiation to anthropogenic decreases in vegetation density. Vegetation density controls both the threshold for fluvial detachment of regolith and the rates of sediment transport by colluvial and fluvial processes. The relative importance of these mechanisms in triggering gully development is not fully understood, however. As such, more research is needed to determine precisely how loss of vegetation triggers gully development in specific cases.

Aside from being an important land-management issue, abrupt fluvial incision has also played an important role in determining the fate of some prehistoric human societies. In the southwestern United States, for example, late Holocene population decline/emigration in Chaco Canyon, New Mexico (Hall, 1977),

and the valley of the Santa Cruz River, Arizona (Waters and Haynes, 2001), coincided with arroyo cutting (i.e., abrupt fluvial incision to create a vertical-walled channel). Proposed factors that led to arroyo cutting include overgrazing/overharvesting, geomorphic response to natural climate change, and the autogenetic behavior of fluvial systems (Antevs, 1952; Cooke and Reeves, 1976; Betancourt, 1990). Despite nearly a century of research, no consensus has emerged as to which factor was dominant. Arroyos are analogous to gullies in that both are vertical-walled channels that are enigmatic in origin, but they differ in that the gullies are generally formed in relatively small (i.e., drainage areas less than ~10 km<sup>2</sup>) upland drainage basins, not the large (greater than ~1000 km<sup>2</sup>) drainage basins where most classic arroyos occur in the southwestern United States. In both cases, better assessment and mitigation of the risk of abrupt fluvial incision under future scenarios of climate and land-cover change require an improved process-based understanding of the geomorphic response to both climatic and anthropogenic perturbations.

## STUDY AREA

In this paper, we constrain the timing and causes for the widespread gullying of hillslopes and low-order fluvial valleys adjacent to the upper Tsangpo Valley, southeastern Tibetan Plateau, using field observations, geochronology, and numerical modeling. We observed deep and repetitive gullying of hillslopes and low-order fluvial valleys in most of the major drainage basins adjacent to the Tsangpo Valley along a transect from Lhasa at 91°E west to Sang Sang at 86°E, a distance of more than 600 km (Fig. 1). The pervasiveness of this gullying is remarkable. Figure 2 illustrates just four examples of many drainage basins in the region where gullying was observed. The sharp breaks in cross-sectional topographic profiles of many of these gullies

<sup>†</sup>E-mail: jdpellet@email.arizona.edu

\*Current address: School of Social Sciences, Humanities and Arts, University of California, Merced, California 95343, USA

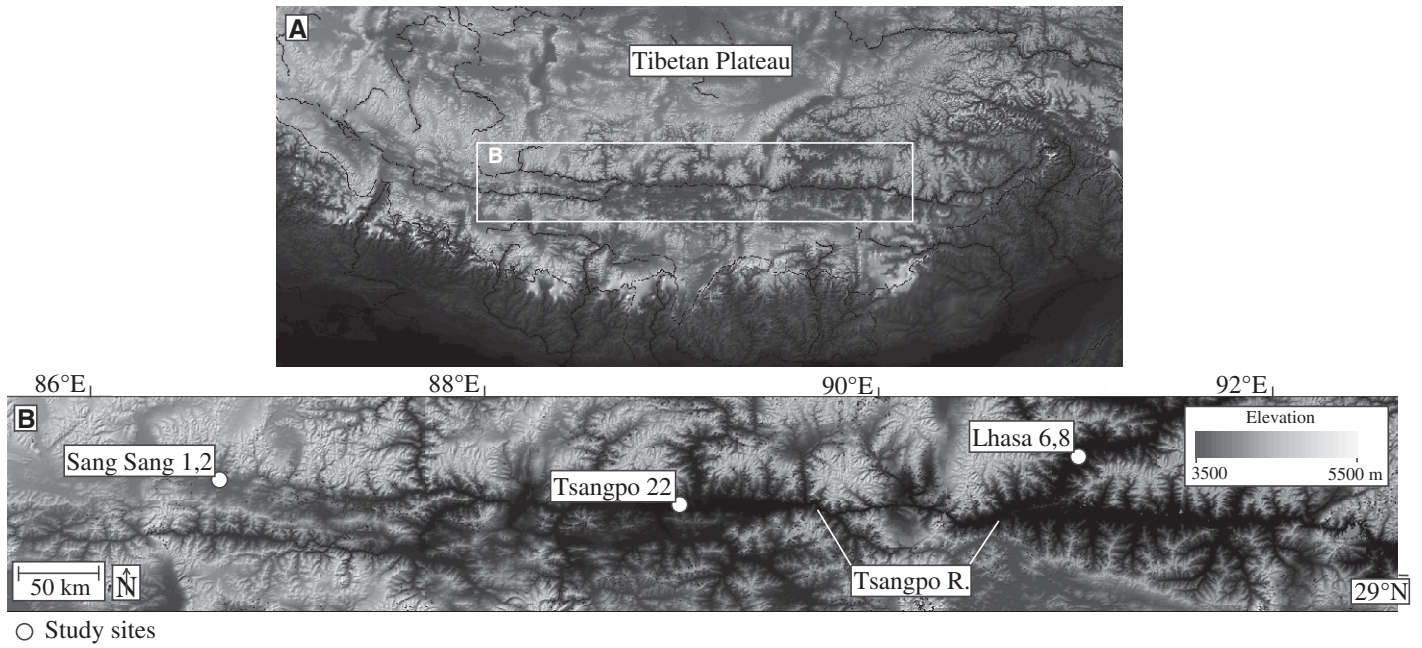


Figure 1. Shaded-relief map of (A) southeastern Tibetan Plateau and (B) study areas along the Tsangpo River Valley.

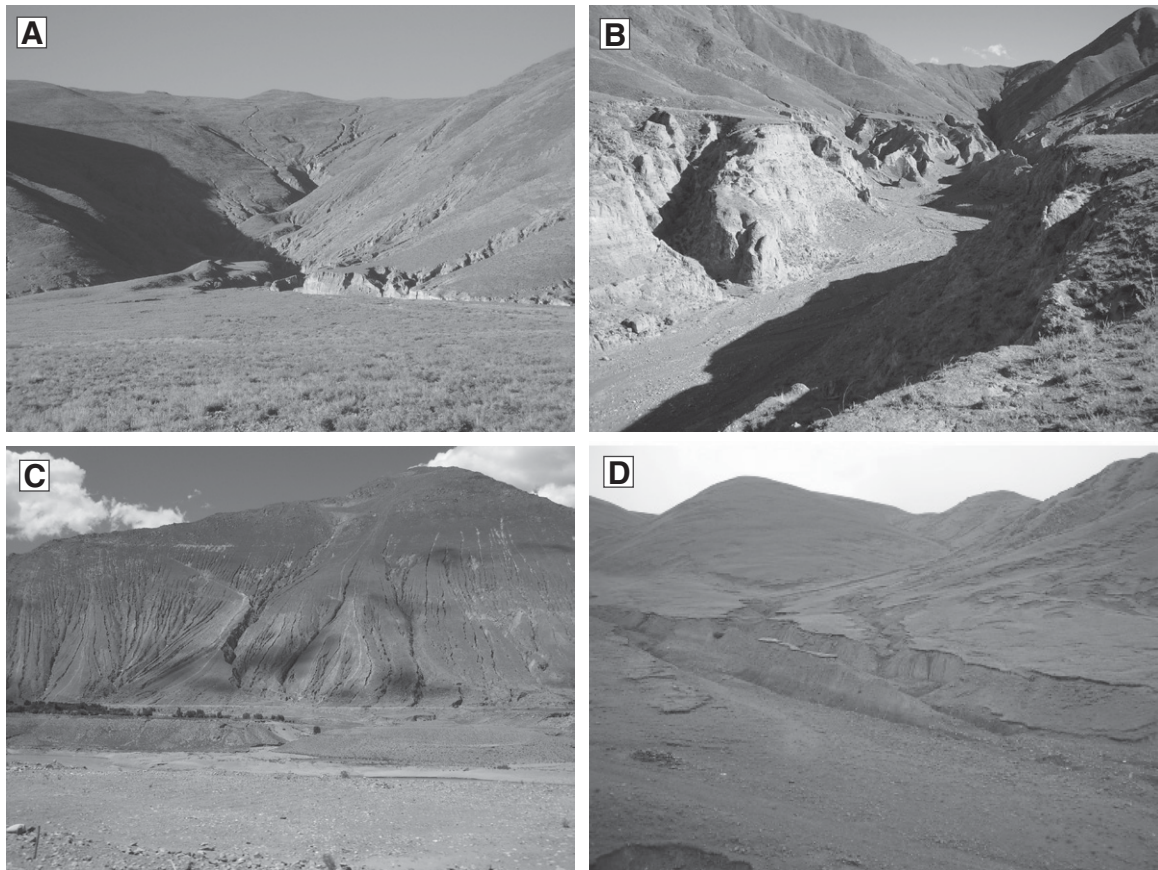


Figure 2. Photographs of typical gullied drainage basins adjacent to the Tsangpo Valley from Lhasa at 91°E west to Sang Sang at 86°E, a distance of 600 km.

suggest that the onset of gullying has been geologically recent. Within individual drainage basins, hillslope segments close to ridge tops are commonly unincised (Fig. 3). Moving downslope, an abrupt, vertical-walled gully head is generally encountered. Farther downslope, a tributary network of gullies coalesces into one or two master gullies where the depth of incision typically reaches a maximum of 5–10 m based on topographic surveys at the five study sites described in this paper. Continuing downslope, the depth of incision decreases toward the base level of the main-stem river (e.g., the Tsangpo River or one of its large tributaries). Figure 3, an aerial photograph of a gullied drainage basin near Lhasa, illustrates the lenticular shape of incision, i.e., increasing and then decreasing depth of incision as one moves downslope through the fluvial system toward the main-stem river. The observation that depth of incision decreases toward the main-stem river is significant because it suggests that gullying in this region is not simply a consequence of tectonic uplift of the Tibetan Plateau or downcutting of the main-stem river. If gullying were the result of tectonic uplift or base-level lowering, it is likely that the depth of

incision would increase rather than decrease toward the main-stem river.

The foot slopes bordering gullied drainage basins are mantled with colluvial, eolian, and alluvial deposits. Gullying of these deposits exposes stacked sequences of buried paleosols, many with stage II+ pedogenic carbonate development (based on the index of Machette, 1985), intercalated with loess. The loess of the upper Tsangpo Valley has a basal age of 13–11 ka and is derived primarily from eolian sorting of glaciofluvial deposits from river valleys in the region (Sun et al., 2007). No buried channel deposits were observed in any of the exposures we examined, and unconformities overlying the paleosols were traceable laterally for hundreds of meters with little or no evidence of erosion. Previous episodes of gully incision can be ruled out based on the absence of channel-fill deposits and unconformities observed in gully exposures. The deposits exposed by gullying represent significant periods of geologic time (at least 10–100 k.y.), based on the extent of pedogenic carbonate development of many of the buried paleosols. Figure 4 illustrates three

typical examples of gully exposures showing stacked sequences of paleosols. These exposures are typical in the sense that we observed similar stacked exposures at 10 sites we visited, but we describe in detail only the five study sites where age control was obtained. Figures 4A and 4B are photographs of gully exposures at our study sites near Lhasa and Sang Sang, respectively, where multiple sequences of reddened paleosols and lighter loess deposits are clearly visible. Figure 4C is a stratigraphic section from our Lhasa 6 site that illustrates the cyclic nature common in these exposures. Five cycles of fining-upward colluvial/alluvial deposits capped by loess are present in this 6 m section. Evidence of pedogenic carbonate accumulation is present in three of the five cycles. The implication of this cyclic nature is that these deposits represent multiple periods of slow aggradation and stability (i.e., soil development).

The study area lies in the high, dry, and cold upper Tsangpo Valley. Sun et al. (2007) summarized the geological setting of this valley from a geomorphic perspective. Mean annual temperatures decrease from around 7 °C in Lhasa (the



**Figure 3.** Aerial photograph of a typical gullied drainage basin adjacent to the Lhasa River (a major tributary to the Tsangpo River) near the city of Lhasa. Note that the depth of incision has a maximum value in the main channel(s) and decreases both upstream (toward channel heads) and downstream toward the junction of the main channel with the Lhasa River (located off of the lower-left corner of the image).

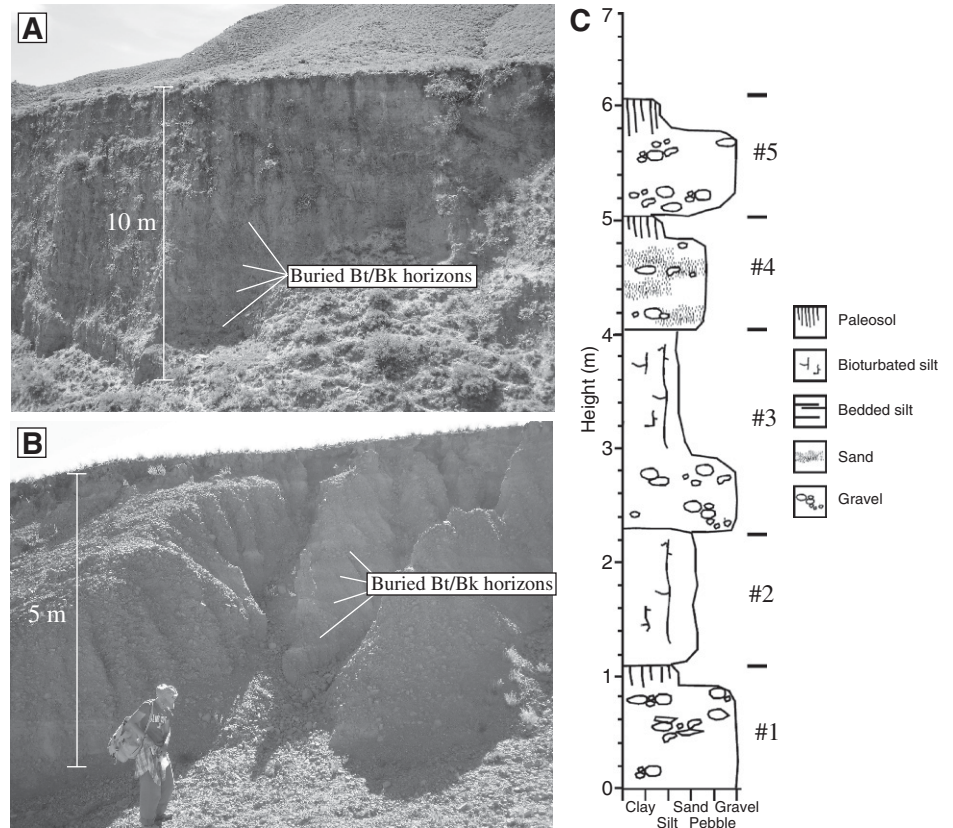


**Figure 4.** Photographs illustrating examples of cyclic colluvial/eolian deposition exposed in gullies near (A) Lhasa and (B) Sang Sang. (C) Stratigraphic section described at the Lhasa 6 study site, illustrating the cyclic nature of deposition and the pedogenesis that commonly caps the fining-upward cycles.

lowest and most easterly sites) to close to 0 °C at higher elevations to the west. Rainfall is highest in Lhasa at 500 mm/yr and decreases steadily to the west to 200 mm/yr near Sang Sang (Institute of Geography, 1999). The slopes of the upper Tsangpo Valley today are covered by cold steppe and shrubland vegetation. In general, vegetation density is higher in the wetter eastern area. Typical xeric shrubs include *Sophora moorcroftiana*, *Leptodermis sauranja*, and *Ceratostigma griffithii*, mixed with an understory of forbs and grasses such as *Stipa bungeana* and *Artemisia webbiana*. Above 4400 m, these species give way to high-cold steppe assemblages dominated by the grass *Stipa purpurea*, mixed with low-lying shrubs such as *Caragana versicolor* (especially westward) (Chang, 1981). The boundary between these shrubland/steppe assemblages and sparse coniferous forest dominated by *Juniperus* and *Cupressus gigantea* currently lies to the east of Lhasa, where rainfall exceeds 500 mm/yr. West of this boundary, a few isolated stands of *Juniperus* are known, which Miehe et al. (2006, 2009) suggested are remnants of once continuous forest cover.

In a series of papers, Miehe and his colleagues (Miehe et al., 2006, 2009; Kaiser et al., 2006, 2009) argued that the current almost treeless landscapes of the southeastern Tibetan Plateau are due to anthropogenic deforestation, i.e., overgrazing/overharvesting. They dated the onset of pastoralism in this region to ca. 8.8 ka using the synchronous occurrence of a rapid decline in forest pollen and the stratigraphic occurrence of pollen clumps, which they interpreted to indicate disturbance by trampling. Miehe et al. (2009) suggested that this deforestation was the trigger for widespread gullying in the region. If correct, it is likely that under the Holocene climate, much of the upper Tsangpo Valley west of Lhasa was once covered by sparse coniferous forest. Holocene forest decline has been documented in many other studies of the eastern and southern Tibetan Plateau, but whether this decline was caused by climate change or human impact is a matter of controversy (Herzschuh et al., 2010). A key goal of this paper is to provide direct age constraints on gully development over a broad geographic region to further test the hypothesis that gullying was triggered by deforestation.

One potential difficulty with the anthropogenic deforestation hypothesis for gully initiation is the fact that climate-change-induced deforestation of the region likely occurred multiple times during the Pleistocene, apparently without causing gully formation, based on the absence of channel-fill deposits in modern gully exposures. During Pleistocene glacial intervals, temperatures on the Tibetan Plateau were ~6 °C

colder than today (Zheng et al., 1998). Such colder temperatures likely caused vegetation to shift to lower elevations in these temperature-stressed alpine biomes. Moreover, the colder temperatures characteristic of Pleistocene glacial intervals coincided with drier conditions, likely stressing plants further. Oxygen isotope data from the speleothem record at Hulu cave near Nanjing (Wang et al., 2001) indicate a strong synchronicity between the strength of the Southeast Asian monsoon (which acts as the dominant source of moisture to the southern Tibetan Plateau) and temperatures in Greenland ice cores. As such, the southern Tibetan Plateau was colder and drier ca. 20 ka. Unfortunately, available constraints on Pleistocene vegetation for the Tibetan Plateau do not pinpoint elevation because they derive from lake cores and, as such, integrate pollen from regions that span a wide range of elevations. Nonetheless, elevation is a critical controlling factor of the geographic ranges of vascular plants in temperature-stressed alpine environments, and it is appropriate to use indirect arguments where direct evidence is lacking. The upper limit of vascular plants today on the southern Tibetan Plateau occurs at ~5 km above sea level (Webster, 1961; Chang, 1981). The upper limit of vascular plants in this region would likely have been ~4 km ca. 20 ka, assuming the widely used lapse rate of 6 °C km<sup>-1</sup> for the Tibetan Plateau (Li et al., 2005) together with the assumption that the upper limit of vascular plants is controlled by temperature. As such, the colder conditions that prevailed during Pleistocene glacial intervals would likely have resulted in an altitudinal shift of coniferous forest broadly similar to that of today. This concept has been incorporated into conceptual models for the Holocene early human occupation of the plateau (Aldenderfer and Zhang, 2004; Aldenderfer, 2007; Brantingham et al., 2007). Any explanation for the initiation of gullying based on anthropogenic deforestation must come to terms with the evidence that hillslopes apparently were not gullied during the naturally deforested conditions of ca. 20 ka and other Pleistocene glacial intervals.

## FIELD OBSERVATIONS AND GEOCHRONOLOGY

### Methods

Our sampling strategy for constraining the age of gully initiation in this region is illustrated schematically in Figure 5. Sites were selected from a broad geographic region extending from Sang Sang (in the west) to Lhasa (in the east) based on their proximity to the major road traversing the upper Tsangpo Valley and the lack

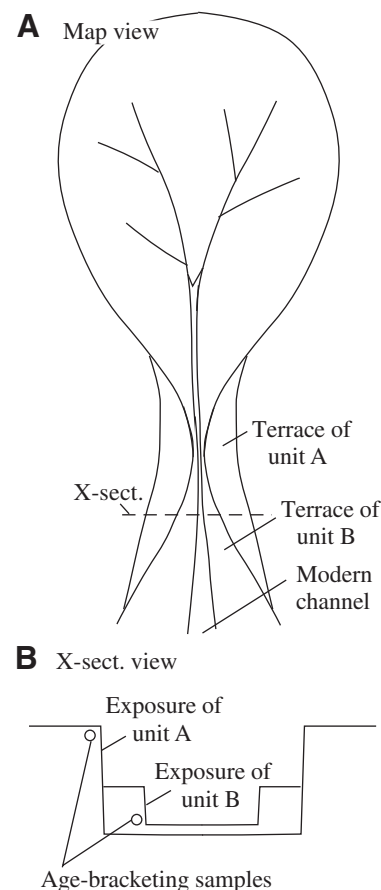


**Figure 5. Schematic diagram illustrating (A) map view and (B) cross-sectional view of the geomorphic/stratigraphic relationships observed in the field and the sampling strategy for constraining the age of gully initiation. At the foot slope of each drainage basin, the landscape has three levels: modern channel (youngest), terrace of unit B (intermediate), and terrace of unit A (oldest). Unit B deposits grade upslope onto the beds of gullied channels. On the fan, the modern channel is incised into unit B deposits. To obtain an optimal bracketing age, we sampled high in the exposure of unit A (to obtain an upper bound age of gully initiation closest to the true age) and low in the exposure of unit B (to obtain a lower bound closest to the true age).**

of other human disturbance. The initiation of gullying cannot be directly dated, but the ages of deposits that predate and postdate the onset of gullying provide bracketing ages. Two terraces are observed at the foot slope of each drainage basin in our study sites. Outside the zone of gullying, modern hillslope deposits grade to the highest terrace, denoted in Figure 5 as the terrace of unit A. Gullying causes incision into this terrace, reworking sediments of unit A

during deposition of unit B, which is therefore inset into unit A. In order to bracket the age of gully initiation, we sampled fine-grained sediments as high as possible in unit A and as low as possible in unit B. The age of sediments in unit A predates the onset of gully, while the age of unit B postdates the onset of gully. We visited 10 localities between Lhasa and Sang Sang with the same basic geomorphic patterns of incision, but we only report in detail here on five sites where age control was obtained. In all the locations that we visited, we observed similar stratigraphic patterns characterized by stacked paleosol sequences with laterally traceable disconformities and an absence of channel-fill deposits.

Before we describe the sample localities in detail, we first describe our methods of optically stimulated luminescence (OSL) sample analysis. Sample preparation was carried out under amber-light conditions. Samples were wet sieved to extract the 90–150  $\mu\text{m}$  fraction and then treated with 1 N HCl to remove carbonates. Quartz grains were extracted by flotation using 2.7 and 2.58  $\text{g cm}^{-3}$  sodium polytungstate solutions, and then they were treated for 75 min in 48% HF, followed by 30 min in 47% HCl. Each sample was rinsed, dried, and resieved, and the <90  $\mu\text{m}$  fraction was discarded to remove residual feldspar grains. The etched quartz grains were mounted on the innermost 2 mm of 1 cm aluminum disks using Silkospray. Chemical analyses were carried out by Chemex Labs, Inc., Sparks, Nevada, using a combination of inductively coupled plasma–mass spectrometry (ICP-MS) and inductively coupled plasma–atomic emission spectrometry (ICP-AES). Dose rates were calculated using the method of Aitken (1998) and Adamiec and Aitken (1998). The cosmic contribution to the dose rate was determined using the techniques of Prescott and Hutton (1994).

Optically stimulated luminescence analyses (Table 1) were carried out on a Riso Automated OSL Dating System Model TL/OSL-DA-15B/C,

equipped with blue and infrared (IR) diodes, using the single aliquot regenerative dose (SAR) technique (Murray and Wintle, 2000). A preheat interval of 260  $^{\circ}\text{C}$  for 10 s was used, with a cut-heat of 220  $^{\circ}\text{C}$ , based upon preheat plateau, dose recovery, and thermal transfer tests between 180  $^{\circ}\text{C}$  and 280  $^{\circ}\text{C}$  (Murray and Wintle, 2003). The decision process of Bailey and Arnold (2006) was used to evaluate all samples for partial bleaching. UNL1537 showed evidence of partial bleaching (skew  $>2\sigma_c$ ), and the minimum age model (MAM; Galbraith et al., 1999) was applied to that sample.  $D_e$  values for all the remaining samples were calculated using the central age model (CAM; Galbraith et al., 1999). At minimum, 40 aliquots were run per sample, with optical ages based upon a minimum of 21 acceptable aliquots. Individual aliquots were monitored for insufficient count rate, poor-quality fits (i.e., large error in equivalent dose,  $D_e$ ), greater than 10% error in the recycling ratio, test dose error greater than 10%, strong medium versus fast component, and detectable feldspar (IR-OSL peak/background greater than 2). Aliquots deemed unacceptable based upon these criteria were discarded from the data set prior to averaging.

## Results

The maximum age of gully at all five locations where age control was obtained ranged from  $4.45 \pm 0.29$  ka to  $8.78 \pm 0.74$  ka, while the minimum age of gully ranged from  $0.58 \pm 0.06$  ka to  $1.61 \pm 0.18$  ka (Table 1). Therefore, the age of initiation of gully is mid-to-late Holocene at all five sites. The age control at one site (Lhasa 6) is ambiguous, however, as explained later herein. Near Sang Sang, we obtained pairs of bracketing ages at two sites we refer to as Sang Sang 1 and 2. At Sang Sang 1, located at  $29^{\circ}24'08.0''\text{N}$ ,  $86^{\circ}43'33.6''\text{E}$  and an elevation of 4643 m, unit A is a 6 m section of sand-dominated alluvial and colluvial deposits atop bedrock of the Shigatse Group shale that

is capped by a 40-cm-thick loess deposit with distinct development of Ao and Bw horizons (following National Resources Conservation Service [NRCS] classification system; Soil Survey Staff, 1975) but shows no significant accumulation of pedogenic carbonate (Fig. 6A). An OSL sample from the loess cap yielded an age of  $6.01 \pm 0.38$  ka (T.06.07.07–01). Downslope, unit A is stratigraphically lower than unit B (Fig. 6A). Unit B includes a loess deposit with pedogenic development, capped by younger sand and gravel deposits. The age of the loess in unit B is  $1.18 \pm 0.09$  ka (T.06.07.07–02). At Sang Sang 2, located at  $29^{\circ}19'25.1''\text{N}$ ,  $87^{\circ}06'21.3''\text{E}$  and an elevation of 4465 m, the top of unit A dates to  $4.69 \pm 0.29$  ka (T.06.07.07–03), and the top of inset unit B dates to  $0.80 \pm 0.06$  ka (T.06.07.07–04). Thus, incision commenced in this area sometime after 5–7 ka and by ca. 1 ka had incised unit A by 3–6 m. Red ceramics were found in unit B at Sang Sang 2, confirming a late Holocene age for unit B (Institute of Archeology, 1999).

Similar field relationships and bracketing ages are observed 600 km to the east at our Lhasa 8 site (Fig. 7). At Lhasa 8, located at  $29^{\circ}45'56.3''\text{N}$ ,  $91^{\circ}27'47.4''\text{E}$  and an elevation of 3754 m, we obtained an OSL age of  $7.25 \pm 0.42$  ka (T.06.07.10–04) on loess at the distal end of the foot slope (unit A) deposits, where the loess thins to less than a meter onto a local alluvial fan. OSL ages from locally inset terraces of unit B yielded an age of  $1.61 \pm 0.18$  ka (T.06.07.10–03). Thus, incision here postdates 7 ka. At Lhasa 6, located at  $29^{\circ}42'20.7''\text{N}$ ,  $91^{\circ}22'34.7''\text{E}$  and an elevation of 3762 m, unit A is characterized by the cyclic aggradation of colluvial and eolian deposits illustrated in Figure 4C. Unit B is characterized by colluvial/alluvial deposits inset into partially eroded older loess deposits (Fig. 7A). The age control at this location is ambiguous because the age relationship observed elsewhere (unit A older than unit B) is reversed, based on our labeling of the samples, with the loess cap of unit A apparently younger

TABLE 1. RESULTS OF OPTICALLY STIMULATED LUMINESCENCE (OSL) ANALYSES

UNL no.	Field no.	Depth (m)	H <sub>2</sub> O (%) <sup>*</sup>	K <sub>2</sub> O (%)	U (ppm)	Th (ppm)	Cosmic (Gy)	Dose rate (Gy/k.y.)	$D_e$ (Gy)	No.	Age (ka)	Skew/ $2\sigma_c$ <sup>†</sup>
1650	T06.07.07-01	0.1	12.8	2.25	2.5	15.8	0.39	$3.48 \pm 0.16$	$20.9 \pm 0.7$	29	$6.01 \pm 0.38$	0.8
1651	T06.07.07-02	0.4	4.3	2.40	1.8	7.9	0.36	$3.19 \pm 0.13$	$3.75 \pm 0.22$	29	$1.18 \pm 0.09$	0.1
1652	T06.07.07-03	0.1	6.4	2.35	3.0	13.8	0.36	$3.74 \pm 0.16$	$17.5 \pm 0.6$	36	$4.69 \pm 0.29$	0.9
1653	T06.07.07-04	0.1	1.2	2.18	2.0	11.1	0.36	$3.40 \pm 0.14$	$2.72 \pm 0.17$	21	$0.80 \pm 0.06$	0.5
1536	T06.07.08-02	0.1	3.4	2.18	1.8	15.9	0.34	$3.59 \pm 0.15$	$31.7 \pm 2.1$	30	$8.78 \pm 0.74$	-0.1
1537	T06.07.08-03	0.1	3.2	2.08	1.5	13.9	0.33	$3.23 \pm 0.13$	$1.88 \pm 0.15$	64	$0.58 \pm 0.06$	3.1
1538	T06.07.10-01	0.1 <sup>§</sup>	3.4	2.83	1.6	10.3	0.31	$3.62 \pm 0.14$	$16.2 \pm 0.1$	31	$4.45 \pm 0.53$	0.3
1539	T06.07.10-02	4.0 <sup>§</sup>	3.2	2.31	2.1	15.5	0.32	$3.70 \pm 0.15$	$3.40 \pm 0.14$	33	$0.79 \pm 0.07$	0.8
1654	T06.07.10-03	0.4	0.4	2.92	2.1	14.8	0.31	$4.28 \pm 0.17$	$6.90 \pm 0.70$	21	$1.61 \pm 0.18$	0.9
1655	T06.07.10-04	0.3	0.7	2.93	2.3	17.3	0.33	$4.52 \pm 0.19$	$32.8 \pm 1.0$	44	$7.25 \pm 0.42$	0.9

<sup>\*</sup>In-situ moisture content.

<sup>†</sup>Minimum age model (MAM; Galbraith et al., 1999) applied if skew  $> 2\sigma_c$  (Bailey and Arnold, 2006) (UNL 1537).

<sup>§</sup>Denotes proposed sample depths based on the assumption that samples at this site were cross-labeled.

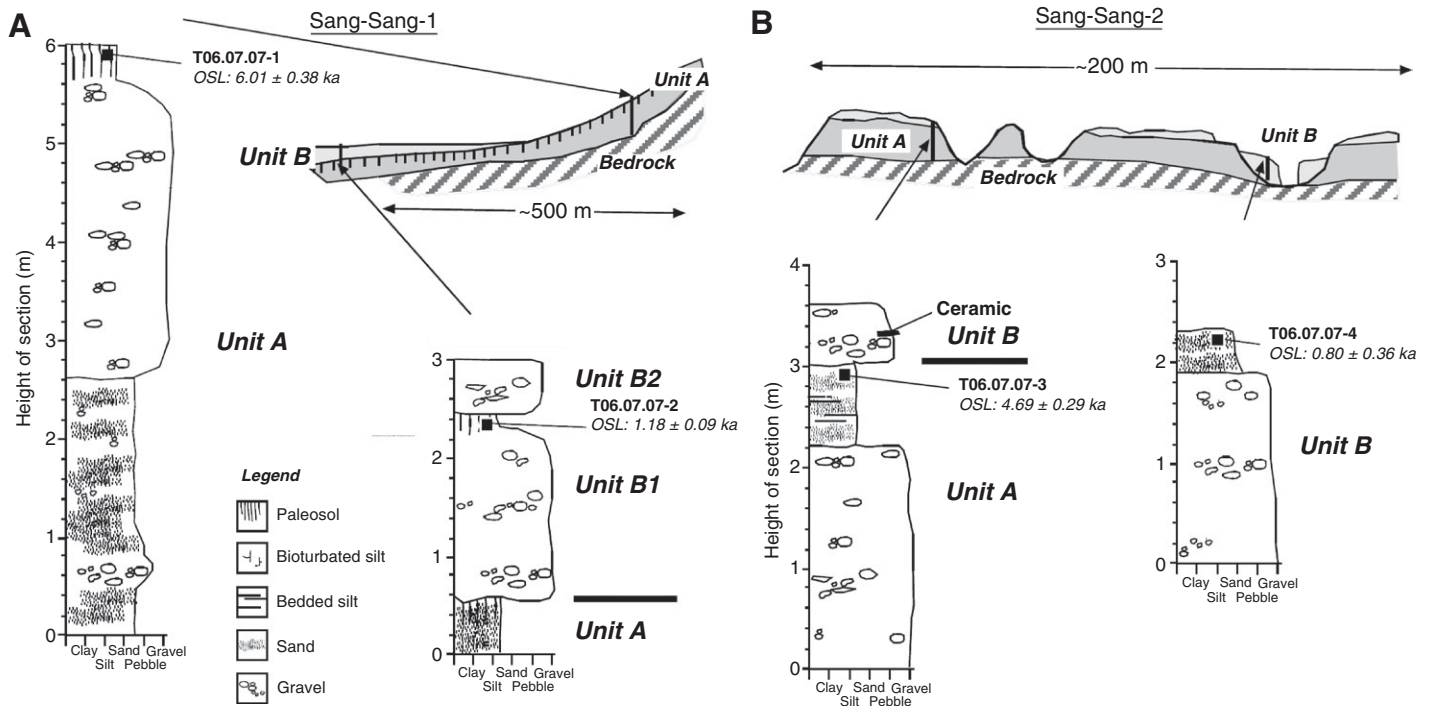


Figure 6. Geomorphic relations and stratigraphic sections of gullied study sites near Sang Sang. (A) Sang Sang 1, (B) Sang Sang 2. See Figure 1 for locations and the text for more description. OSL—optically stimulated luminescence.

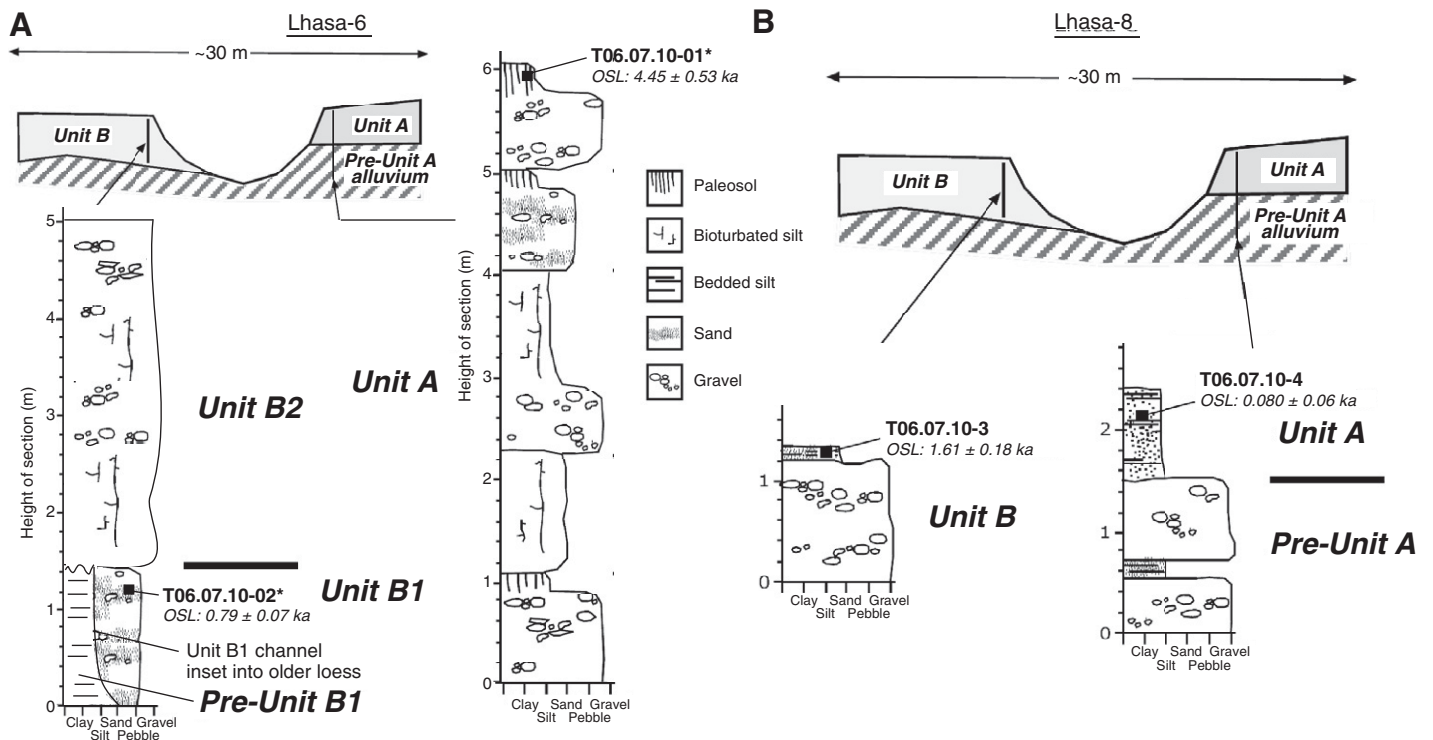


Figure 7. Geomorphic relations and stratigraphic sections of gullied study sites near Lhasa. (A) Lhasa 6, (B) Lhasa 8. Asterisks next to the sample IDs at Lhasa 6 indicate that these are proposed dates based on the assumption that the samples were cross-labeled at this site. See Figure 1 for locations and the text for more description. OSL—optically stimulated luminescence.

(at  $0.79 \pm 0.07$  ka; T.06.07.10–02) than the base sediments of the stratigraphically inset unit B ( $4.45 \pm 0.53$  ka; T.06.07.10–01). The samples at this site were most likely cross-labeled in the field, based on the presence of a pedogenic stage II–III development in the loess cap of unit A and the alluvial sediments immediately below the loess. As such, Figure 7A reports proposed ages of  $4.45 \pm 0.53$  ka for unit A and  $0.79 \pm 0.07$  ka for unit B. Alternatively, it is possible that the loess cap of unit A is unrelated to incision and that the age of unit B sediments are unusually old at this one site. In either case, the ages at Lhasa 6 are consistent with the initiation of gullying in the mid-to-late Holocene. Between Sang Sang and Lhasa, we obtained bracketing dates of  $8.78 \pm 0.74$  ka in unit A (T.06.07.08–02) and  $0.58 \pm 0.06$  ka in unit B (T.06.07.08–03) at a site (Tsangpo 22, located at  $29^{\circ}19'04.6''\text{N}$ ,  $88^{\circ}56'51.6''\text{E}$  and an elevation of 3876 m) with similar depositional units and bounding terraces as Lhasa 8 and Sang Sang 1 and 2. The similar age bracket for gullying at the Tsangpo 22 site lends further confidence that the mid-to-late Holocene age of gullying is regionally applicable, despite the ambiguity posed by the apparent stratigraphic age reversal at Lhasa 6.

## NUMERICAL MODELING

### Motivation

The morphology of soil-mantled landscapes is controlled by a competition between colluvial processes, which tend to smooth the landscape, and fluvial processes, which tend to incise the landscape. In order for fluvial processes to occur on a given landscape, a detachment or entrainment threshold must also be exceeded. As such, soil-mantled landscapes are controlled by three fundamental parameters: a detachment/entrainment threshold, a parameter that quantifies the rate of colluvial transport per unit slope gradient, and a parameter that controls the rate of fluvial erosion for a given contributing area and channel gradient. Field work by Graf (1979) and Prosser and his colleagues (Prosser and Slade, 1994; Prosser and Dietrich, 1995; Prosser and Soufi, 1998) concluded that the location where a valley begins is primarily controlled by the detachment threshold. Prosser and Dietrich (1995), for example, concluded from field experiments that valleys begin where a threshold shear stress is exceeded. That perspective informed the work of Rinaldo et al. (1995), who assumed that the impact of climate variability on valley density could be quantified by varying the detachment threshold, not the rates of colluvial and fluvial processes above that threshold. Recent research has shown, however, that the spacing

and morphology of low-order fluvial valleys are controlled primarily by a competition between rates of colluvial deposition and fluvial erosion (Howard, 1994; Perron et al., 2008, 2009). This perspective suggests that the relative values of colluvial and fluvial sediment transport are as important or more important than the value of the detachment threshold in controlling where valleys begin and the morphology of soil-mantled landscapes generally. In this section, we test the related hypothesis that *changes* in the relative rates of colluvial and fluvial sediment transport from a near-equilibrium condition can cause valleys to infill (if rates of fluvial scour decrease relative to colluvial deposition) or incise (if rates of fluvial scour increase relative to colluvial deposition). If incision is sufficiently rapid, gullies may form.

### Methods

The classic approach to modeling the evolution of soil-mantled hillslopes of moderate relief is the diffusion equation (Culling, 1960, 1963):

$$\frac{\partial z}{\partial t} = D\nabla^2 z, \quad (1)$$

where  $z$  is the elevation of the land surface,  $t$  is time, and  $D$  is diffusivity.  $D$  quantifies the rate of colluvial transport per unit hillslope gradient. On steep slopes close to the angle of stability, it is necessary to modify Equation 1 to include the effects of nonlinear slope-dependent colluvial transport (Roering et al., 1999). Hillslopes take on a range of gradients in the drainage basins adjacent to the upper Tsangpo Valley, but steep slopes where nonlinear slope-dependent transport is significant are limited to a relatively small fraction of the total study area. Based on an analysis of slopes computed from a 90 m/pixel Shuttle Radar Topography Mission (SRTM) digital elevation model, 32% of the area of drainage basins adjacent to the upper Tsangpo Valley has gradients of  $20^{\circ}$  or higher and only 17% has gradients of  $30^{\circ}$  or higher. As such, we adopt the linear-slope-dependent (i.e., diffusion) approximation for colluvial sediment transport in our model, recognizing that this approximation breaks down for a subset of the drainage basins in the study area.

The slopewash/fluvial erosion of regolith and colluvium may involve transport-limited and/or detachment-limited conditions, depending on the surficial characteristics and the texture of the eroding regolith (Willgoose, 2005). Models in the geomorphic literature have often treated the slopewash/fluvial erosion of regolith as purely transport limited or purely detachment limited, however. The models of Smith and Bretherton

(1972), Willgoose et al. (1991), Tarboton et al. (1992), Tucker and Bras (1998), Istanbuloglu et al. (2003), and Simpson and Schlunegger (2003), for example, treated regolith erosion as purely transport limited, while those of Howard (1994), Rinaldo et al. (1995), Moglen and Bras (1995a, 1995b), and Perron et al. (2008, 2009) treated regolith erosion as purely detachment limited. The key assumption of detachment-limited models is that sediment is transported predominantly as suspended load and, hence, that fluvial deposition can be neglected. Conversely, transport-limited models assume that sediment is transported predominantly as bed load. In our study sites in the southeastern Tibetan Plateau, we observed primarily colluvial and eolian deposits in gully-exposed stratigraphies, and the occurrence of alluvial deposits (characterized by the presence of bedding and well-sorted sediments) was negligible on hillslopes and low-order valleys but became a significant component of the total deposit thickness near the foot slope of each drainage basin. In addition, much of the regolith in this region is composed of relatively fine-grained (i.e., fine sand, very fine sand, and silt) eolian sediments. For these reasons, we adopted a detachment-limited model for the slopewash/fluvial erosion of regolith in this paper. As noted already, alluvial deposits are present in the foot-slope deposits, but given that foot-slope deposits comprise a relatively small area within each drainage basin, we regard a detachment-limited model to be the most appropriate model for the drainage basins as a whole in our study sites. In this regard, it should be emphasized that valley fills, such as those illustrated in Figure 2, need not necessarily contain slopewash/fluvial deposits. In soil-covered landscapes, valleys can become filled predominantly with colluvial deposits, particularly in the low-order valleys that are the focus of this paper. If the rate of slopewash/fluvial erosion equals the rate of colluvial deposition plus the rate of rock uplift relative to base level, an approximate equilibrium condition exists. Perturbations from that equilibrium (in which the relative rates of fluvial erosion and colluvial deposition change) can trigger valley filling or incision depending on the direction of change.

Combining Equation 1 with a detachment-limited model for the fluvial erosion of regolith yields (Howard, 1994; Perron et al., 2008, 2009)

$$\begin{aligned} \frac{\partial z}{\partial t} &= D\nabla^2 z - K(A^m S^n - \theta_c) + \frac{\rho_r}{\rho_s} U \text{ if } A^m S^n > \theta_c \\ &= D\nabla^2 z + \frac{\rho_r}{\rho_s} U \text{ if } A^m S^n \leq \theta_c, \end{aligned} \quad (2)$$

where  $K$  is an erodibility coefficient for the regolith,  $A$  is contributing area,  $S$  is along-channel

slope,  $\theta_c$  is a detachment threshold,  $\rho_r/\rho_s$  is the ratio of rock to sediment density, and  $U$  is the rock uplift rate relative to base level. It should be noted that Equation 2 is not the only formulation of the stream-power model for soil-mantled landscapes, but this form follows two landmark references (e.g., Howard, 1994; Perron et al., 2008). Here, we adopt the common assumption that the exponents  $m$  and  $n$  are 0.5 and 1, respectively. Assuming these values for  $m$  and  $n$ ,  $K$  has units of one over time, and  $\theta_c$  has units of length. Slope-area relationships of detachment-limited fluvial channels suggest that the ratio  $m/n$  is in the range of 0.3–0.5 (e.g., Hack, 1957; Ijjasz-Vasquez and Bras, 1995; Whipple, 2004). The absolute values of  $m$  and  $n$  are less well constrained, but repeat field surveys of a rapidly eroding landscape by Howard and Kerby (1983) support an approximately linear relationship between erosion rate and along-channel slope. A value of  $m$  equal to 0.5 is consistent with a linear scaling between discharge and drainage area. This is consistent with data available relating discharge  $Q$  and contributing area  $A$  at spatial scales less than 10 km<sup>2</sup>. In Goodrich et al. (1997),  $Q$  was found to be almost linear with  $A$  at these scales, despite the fact that their study was located in a semiarid region, where  $Q$  versus  $A$  deviates substantially from a linear relationship at larger spatial scales. Discharge increases more linearly with contributing area at small spatial scales because infiltration losses are minimal during large runoff events at these scales.

The numerical model of this paper is a finite-difference implementation of Equation 2. The model begins at time zero with an initial topography that includes a gently sloping plane toward the base level with small (1 m root-mean-squared) white-noise variations in topography to seed the initial valley incision. The inclined plane is needed to establish channels draining toward the base level. The random noise is needed so that valleys will not be artificially straight and because there is always some heterogeneity in initial topography or substrate erodibility, and the initial noise represents that variability. The contributing area  $A$  is calculated during each time step of the model using the  $D_\infty$  algorithm of Tarboton (1997), which partitions the contributing area entering each pixel (a proxy for water discharge) between the two adjacent neighbors for which the triangular facet (formed by intersection with the center pixel) has the steepest gradient. The slopewash/fluvial erosion component of Equation 2 is solved for at each time step of the model by calculating the along-channel slope in the downslope direction (also referred to as upwind differencing) using a time step that guarantees numerical stability. The diffusion term in Equation 2 is calculated using an implicit numerical method that is stable for all time steps. In the model, drainage basin upslope and side-slope boundaries were assumed to be divides (i.e., no flux boundary conditions were applied), and the downstream boundary was assumed to be a fixed elevation

(as is appropriate for a valley-floor channel capable of transporting all of the sediment delivered from the drainage basin).

As a baseline condition from which to perturb the landscape, we constructed a landscape with an approximately steady-state or equilibrium condition with length 500 m, width 250 m, and pixel size of 2 m, i.e., comparable to the size of drainage basins in our study sites (Fig. 8A) and based on the comparison in Figure 9. It should be noted that assuming a landscape in approximate equilibrium prior to the initiation of gullying does not coincide precisely with the actual conditions of this landscape based on field observations. Field observations suggest that slow ( $\sim 1$  cm k.y.<sup>-1</sup>) aggradation has occurred in valleys throughout much of the Quaternary, switching to fast ( $\sim 1$  m k.y.<sup>-1</sup>) fluvial incision in the mid-to-late Holocene. The  $\sim 1$  cm k.y.<sup>-1</sup> order-of-magnitude estimate is based on  $\sim 1$  m of predominantly colluvial and eolian deposition between episodes of paleosol development and the assumption that each paleosol represents a single glacial-interglacial sequence of  $\sim 100$  k.y. Of course, the equilibrium assumption for the model landscape prior to perturbation is an idealization, but based on the fact that aggradation prior to perturbation was likely two orders of magnitude slower than incision following perturbation, it is a reasonable approximation in this case.

The approximately steady-state landscape used as input to the perturbation experiments was generated using a constant, uniform value

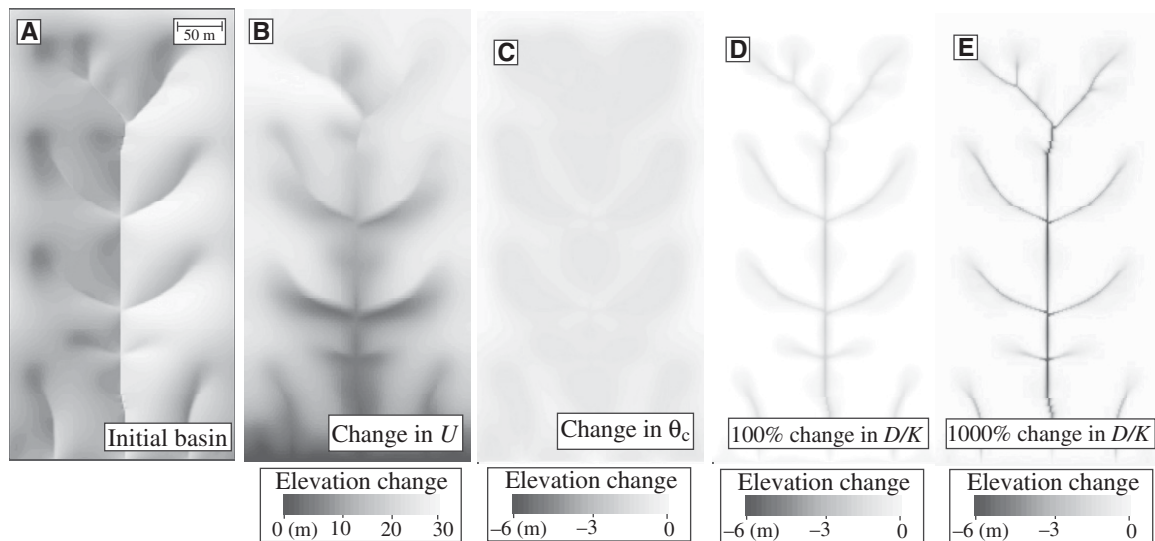
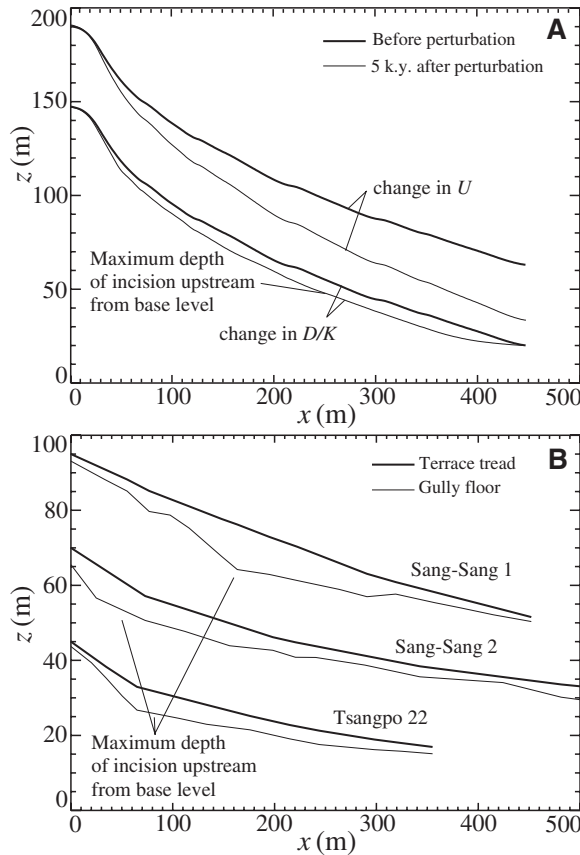


**Figure 8.** Model topography (A) before and (B–E) after abrupt changes in the model parameters. (A) Shaded-relief image of the steady-state drainage basin produced by numerical model with  $(\rho_r/\rho_s)U = 0.05$  m k.y.<sup>-1</sup>,  $D = 3$  m<sup>2</sup> k.y.<sup>-1</sup>,  $K = 0.1$  k.y.<sup>-1</sup>, and  $\theta_c = 10$  m after 10 m.y. of uplift relative to base level (lower boundary). (B–E) Grayscale maps of the difference in elevation between the model topography before and after the change in each parameter. Changes in the values of  $D$  and/or  $K$  lead to localized incision (gullying) most similar to that observed in our study sites along the Tsangpo Valley.

**Figure 9.** Comparison of the longitudinal profiles of gullies (A) predicted by the numerical model and (B) observed at three of our five study sites. Thick curves represent the profile of the main channel terrace above the gully floors. Thin lines represent the gully floors. Profiles in A illustrate that tectonic/uplift rate perturbations lead to a maximum incision depth at the basin outlet. Perturbations in  $D$  and/or  $K$  lead to maximum incision depths upslope from the basin outlet. Observed profiles have a maximum depth of incision upstream from the drainage basin outlet, a pattern most consistent with the model prediction corresponding to a change in  $D$  and/or  $K$ .



of  $(\rho_r/\rho_s)U = 0.05 \text{ m k.y.}^{-1}$  for 10 m.y. This value for  $(\rho_r/\rho_s)U$  is consistent with exhumation rates from the Tibetan Plateau, which are  $\sim 0.05 \text{ m k.y.}^{-1}$  (Rohrman et al., 2008). The 10 m.y. period is a sufficiently long time for the landscape to steepen in response to tectonic uplift, such that an approximately steady-state balance is achieved between rock uplift and erosion. Some valley and ridge migration continues to occur in this model even after an approximately steady-state condition has been achieved, but the surface elevation changes are limited to less than 1 m over a 10 k.y. period. The remaining parameter values were set to be  $D = 3 \text{ m}^2 \text{ k.y.}^{-1}$ ,  $K = 0.1 \text{ k.y.}^{-1}$ , and  $\theta_c = 10 \text{ m}$ . The value of  $D$  was chosen as an intermediate value based on values reported in the literature, with  $D \sim 1 \text{ m}^2 \text{ k.y.}^{-1}$  characteristic of arid and semiarid climates, and  $D \sim 10 \text{ m}^2 \text{ k.y.}^{-1}$  characteristic of mesic climates based on the review by Hanks (2000). Given a rock uplift rate and a diffusivity value, the relief and valley density of the model landscape in steady state are a function of  $K$  and  $\theta_c$ . The values  $K = 0.1 \text{ k.y.}^{-1}$  and  $\theta_c = 10 \text{ m}$  were chosen because they yielded a model landscape with relief (130 m) and average hillslope length ( $\sim 50 \text{ m}$ , the average downslope distance from a point

on the hillslope to the nearest channel) comparable to those in our study sites based on the comparison in Figure 9.

**Results**

The equilibrium landscape produced by the model after 10 m.y. of uplift was input into a series of numerical experiments in which the values of each of the model parameters were perturbed in order to determine the geomorphic response to changes in each parameter. We systematically perturbed the landscape by separately changing the values of  $(\rho_r/\rho_s)U$ ,  $D$ ,  $K$ , and  $\theta_c$  and examined the landscape response over time scales appropriate for each perturbation. First, we consider the landscape response to a step change in  $(\rho_r/\rho_s)U$ . Figure 8B illustrates the change map between the initial landscape of

Figure 8A and the same landscape 500 k.y. after a step change in  $(\rho_r/\rho_s)U$  from  $0.05 \text{ m k.y.}^{-1}$  to  $0.1 \text{ m k.y.}^{-1}$  by doubling the value of  $U$  (listed as perturbation 1 in Table 2). Increasing the uplift rate in this way causes a knickpoint to form at the basin outlet that propagates upslope through the main channel and its tributaries over time. Zones that appear black in Figure 8B (i.e., the lower portion of the basin) have incised relative to the areas in white. Plots of the longitudinal profile of the main valley before and after the increase in uplift rate (Fig. 9A) illustrate that the maximum depth of incision occurs near the outlet where the drainage basin meets the valley-floor channel. The magnitude of the incision near the outlet depends on the relative change in  $(\rho_r/\rho_s)U$ , but in all cases, an increase in  $(\rho_r/\rho_s)U$  results in a maximum depth of incision located at the basin outlet. This model result corroborates the conceptual model (discussed in the Introduction) that tectonic uplift and/or base-level fall triggers incision that increases continuously toward the main-stem river. Similar results can be obtained by lowering the base-level elevation abruptly rather than increasing the uplift rate of the basin. The model prediction that the maximum depth of incision occurs at the basin outlet is inconsistent with the observation, illustrated in Figures 3 and 9B, that the maximum depth of incision occurs upstream from where the main tributary valley meets the valley-floor channel. Longitudinal profiles and depths of gully incision obtained at three of our five study sites by field survey, plotted in Figure 9B, illustrate that the greatest incision occurs upstream from where the main tributary valley meets the Tsangpo River. We conclude that it is unlikely that base-level lowering of the Tsangpo River could have caused this gullying.

Next, we consider the effect of a step change in the detachment threshold  $\theta_c$ . Figure 8C illustrates the change map between the initial landscape of Figure 8A and the same landscape 5 k.y. after a step change in  $\theta_c$  from 10 m to 1 m (listed as perturbation 2 in Table 2). When considering the effects of a change in  $D$ ,  $K$ , or  $\theta_c$ , the landscape responds more quickly than for a step change in  $U$  (the effects of which accumulate over time). As such, we chose 5 k.y. as an appropriate time scale over which to examine the response of the valley system to a change in

TABLE 2. MODEL PARAMETERS USED IN THE NUMERICAL EXPERIMENTS

	$(\rho_r/\rho_s)U$ ( $\text{m k.y.}^{-1}$ )	$D$ ( $\text{m}^2 \text{ k.y.}^{-1}$ )	$K$ ( $\text{k.y.}^{-1}$ )	$\theta_c$ (m)	Duration (m.y.)
Equilibrium	0.05	3	0.1	10	10
Perturbation 1	0.10	3	0.1	10	0.005
Perturbation 2	0.05	3	0.1	1	0.005
Perturbation 3	0.05	1.5	0.1	10	0.005
Perturbation 4	0.05	0.3	0.1	10	0.005

$D$ ,  $K$ , and  $\theta_c$ . Hillslopes can require 10–100 k.y. or more to completely adjust to changes in tectonic or climatic forcing conditions, but here we focus on the valley response over a time scale comparable to the mid-late Holocene time scale for gully development constrained by our OSL dates. In all of these cases, the valley system fully responded to the perturbation over the 5 k.y. time scale, incising or not incising as the conditions dictated. The change map in Figure 8C illustrates that the drainage basin responds to an abrupt lowering of  $\theta_c$  by stripping ~1 m of regolith uniformly from areas upslope of each valley head. The result of this erosion is a change map characterized by a light-gray color throughout much of the drainage basin. Note that the main valley(s) does(do) not exhibit significant fluvial erosion, however. To interpret this result, note that varying the value of  $\theta_c$  affects the rate of fluvial erosion most significantly in the vicinity of valley heads, where fluvial erosion is roughly in balance with diffusive infilling. Decreasing the value of  $\theta_c$  in this region causes valley heads to branch and migrate headward, causing significant erosion upslope from each valley head. Erosion is diffuse rather than localized, however, because of the importance of the diffusive term in Equation 2 in the vicinity of valley heads. In the main valleys, however, the product  $A^{1/2}S$  is much greater than  $\theta_c$ , and therefore a decrease in the value of  $\theta_c$  results in relatively little change in the rate of erosion. As a result, significant localized incision of the main valleys (i.e., gullying) may not result from a decrease in the value of  $\theta_c$  alone.

Decreasing the value of  $D$  and/or increasing the value of  $K$  are shown to trigger gully development, however, as illustrated in Figures 8D and 8E. Here, we consider the effects of lowering the value of  $D$  only, but similar results are obtained by increasing the value of  $K$  by the same proportion. Figure 8D illustrates the change map between the initial landscape of Figure 8A and the same landscape 5 k.y. after a 100% step change in  $D$  from  $3 \text{ m}^2 \text{ k.y.}^{-1}$  to  $1.5 \text{ m}^2 \text{ k.y.}^{-1}$  (listed as perturbation 3 in Table 2). This change map illustrates that the basin responds by incising along the main valleys. The greatest incision (3 m in this case) occurs some distance upstream from the basin outlet (Fig. 9A). The incisional response to changes in  $D$  is in proportion to the magnitude of change, as illustrated by the deeper incision that results from an order-of-magnitude change in  $D$  (Figs. 8E and 9A). Figure 8E illustrates the basin response to a change in  $D$  from  $3 \text{ m}^2 \text{ k.y.}^{-1}$  to  $0.3 \text{ m}^2 \text{ k.y.}^{-1}$  (listed as perturbation 4 in Table 2). In this case, the depth of incision reaches a maximum of 6 m (longitudinal profile shown in Fig. 9A), i.e., twice that of the incision result-

ing from the smaller, 100% change in  $D$ . The observation that the maximum depth of incision (3–6 m) predicted by the model is on the same order as the observed depth of incision at our study sites provides confidence in the parameter values used in these numerical experiments.

## DISCUSSION

An advantage of a landform evolution model based on Equation 2 is that it is governed by just four parameters. The disadvantage of the model is that the relationships among climate, land use, and the parameters  $D$ ,  $K$ , and  $\theta_c$  are not precisely known. Nevertheless, associations among runoff, vegetation cover, and the values of  $D$ ,  $K$ , and  $\theta_c$  are sufficiently well constrained for the model to be used to qualitatively evaluate the feasibility of alternative hypotheses for gully development. Two lines of evidence suggest that the value of  $D$  increases in areas of higher vegetation density. First, Hanks (2000) compiled data on values of  $D$  inferred from the degradation of landforms of known age (e.g., pluvial shoreline scarps). The inferred values of  $D$  increase in more mesic climates, i.e., they are in the range of  $0.1\text{--}0.7 \text{ m}^2 \text{ k.y.}^{-1}$  in the hyperarid and arid portions of Israel, in the range of  $0.5\text{--}2.0 \text{ m}^2 \text{ k.y.}^{-1}$  in the arid and semiarid portions of the western United States, and equal to or greater than  $\sim 10 \text{ m}^2 \text{ k.y.}^{-1}$  in coastal California and Michigan. Second, Hughes et al. (2009) inferred a near doubling of colluvial transport in a landscape of moderate relief in New Zealand between the late Pleistocene and early Holocene, coincident with a shift to a forest ecosystem (e.g., a higher vegetation density) in the Holocene. The results of Hughes et al. (2009) are consistent with a series of papers that relate the value of  $D$  directly to vegetation density (Roering et al., 2004; Walther et al., 2009). Rates of sediment transport by bioturbation can be expected to increase with increasing vegetation density because more plants are available to drive sediment transport.

The value of  $K$  is the rate of fluvial erosion above the threshold condition, normalized for the effects of contributing area and slope. Several lines of evidence suggest that the value of  $K$  increases with decreasing vegetation density. Studies performed over the past six decades suggest that a key role played by vegetation is to protect the underlying ground surface from rain splash, thus decreasing the amount of sediment transported by overland flow. Rain splash can be effective at disaggregating and detaching soil particles from portions of the landscape that are not covered by leaves, stones, or other obstructions. Experiments illustrate that overland flow produced from rainfall can be responsible for orders-of-magnitude more sediment trans-

port than overland flow without rainfall (e.g., Ekern, 1951; Rose, 1960; Gabet and Dunne, 2003). Such experiments imply that rain splash greatly reduces the cohesion and aggregation of sediment prior to transport by overland flow. Evidence also suggests that vegetation roots increase the cohesion of regolith (e.g., Prosser and Dietrich, 1995). Such studies suggest that higher vegetation density increases the detachment threshold  $\theta_c$ . Tucker et al. (2006), for example, compiled data from the literature on the critical shear stress required for the detachment of soil from hillslopes. These authors reported that the critical shear stress can vary from a few Pascals (for unvegetated, disturbed regolith) to a few hundred Pascals (for uniformly grass-covered regolith). A key role of vegetation in influencing erosion may also occur via the partitioning of water among runoff, infiltration, and evapotranspiration, i.e., a higher vegetation density results in less runoff for the same precipitation. This latter mechanism also implies an inverse relationship between vegetation density and the value of  $K$ . These different mechanisms for vegetation-erosion coupling are not mutually exclusive, and the primary mechanism by which vegetation controls fluvial erosion rates is likely to vary from one landscape to the next depending on relief and substrate texture (e.g., the fluvial erosion of rain splash-detached sediments is likely more important in fine-grained regolith/colluvium than coarse-grained regolith/colluvium). At present, there is no consensus within the geomorphic community on which of these three mechanisms is most important in controlling the vegetation-erosion relationship for any one specific landscape. However, regardless of whether vegetation controls erosion primarily via protection from rain splash, an increase in soil cohesion from roots, or by increasing evapotranspiration, evidence suggests that  $K$  varies inversely with vegetation density, and  $\theta_c$  varies directly with vegetation density. It should also be noted that several landscape evolution modeling studies have explored the relationship between fluvial erosion and vegetation more explicitly than the approach we use here (e.g., Collins et al., 2004; Istanbuluoglu et al., 2004; Istanbuluoglu and Bras, 2005). However, until better constraints exist on the relative importance of different mechanisms for vegetation-erosion coupling (including, e.g., leaf protection from rain splash vs. root protection from detachment), it is appropriate to use a simplified erosion model (e.g., Equation 2) together with available constraints on the way in which each parameter is controlled by vegetation density.

In order to understand conceptually how a decrease in  $D$  or increase in  $K$  can cause gullying, it is important to note that when a steady-

state condition is achieved prior to decreasing the value of  $D$  or increasing the value of  $K$ , the morphology of the landscape is determined by a balance between colluvial infilling of sediment from hillslopes into valleys and the fluvial excavation of that sediment from valleys. A decrease in the value of  $D$  causes a reduction in the rate of colluvial transport into valleys. Since the elevation of the valley bottom is controlled by a balance between the rate of infilling and the rate of excavation, a decrease in  $D$  with no corresponding decrease in  $K$  will cause an imbalance between infilling and excavation that may result in lowering of the valley bottom, i.e., incision or gully. Similarly, if  $D$  remains constant and the rate of fluvial excavation increases, incision may also occur.

The results of this paper provide a preliminary mechanistic basis for understanding how tributary drainage basins of the upper Tsangpo River were gullied in the mid-to-late Holocene. Human-caused devegetation would likely have decreased  $\theta_c$  and  $D$  while likely increasing  $K$ , based on the discussion of the way in which vegetation controls these parameters. If gullying began in the mid-Holocene (i.e., near the earliest portion of the age brackets reported here), the value of  $K$  would have been still higher due to the wetter conditions that prevailed on the Tibetan Plateau at that time (Huang et al., 2009). As the numerical model illustrates, these changes would have combined to yield shallow but extensive erosion upslope from first-order channels (associated with the decrease in  $\theta_c$ ) and localized downcutting in the main valley(s) (associated with decreases in  $D$  and increases in  $K$ ). During late glacial time, devegetation would have also lowered  $D$  relative to interglacial conditions. However, it is likely that the value of  $K$  would have also been relatively low compared to mid-to-late Holocene conditions due to the drier conditions characteristic of late glacial time. Given that incision can be caused by a decrease in  $D$  or an increase in  $K$ , we propose that the geomorphic response to the decrease in  $D$  caused by the climatically triggered devegetation in late glacial time was likely accompanied by a simultaneous decrease in  $K$ . Available constraints on the strength of the Asian monsoon indicate that the Tibetan Plateau would have been significantly drier in late glacial time compared to today (Wang et al., 2001) and much drier than the mid-Holocene. Without more runoff, the rates of fluvial excavation (i.e.,  $K$  values) required to trigger incision would not have occurred despite a decrease in  $D$ . Other factors may have also contributed to landscape stability during Quaternary glacial intervals. For example, the relatively high rates of loess deposition, which occurs throughout the landscape but was

likely higher in valley bottoms compared to side slopes and interfluvies, may have counteracted the decrease in the colluvial transport of sediment into valleys at those times.

The numerical model used in this paper illustrates that gullying was likely triggered by a decrease in the rate of colluvial transport into channels and/or an increase in the rate of fluvial excavation associated with devegetation. Vegetation density impacts both sides of this balance because less vegetation results in lower rates of colluvial transport into channels as well as more and faster runoff, thus resulting in higher rates of fluvial erosion. Interestingly, the model illustrates that gullying is not simply a result of a decrease in the threshold for detachment, although a decrease in the detachment threshold was likely responsible for some of the soil stripping that we observe. Model results suggest that decreasing the detachment threshold strips soil from hillslopes above channel heads, but it does not, in and of itself, lead to gully. The numerical model of this paper is an idealized representation of a very complex system, however, and limitations of the model should be noted. Most important, there is the fact that fluvial erosion rates in the model are represented in an approximate way using the product of the local slope gradient, the square root of contributing area, and the empirical coefficients  $K$  and  $\theta_c$ . This approach fails to fully represent the increased hydrologic response of the drainage basin as gullies develop. In nature and in the numerical model, devegetation triggers valley incision by modifying the balance between colluvial infilling and fluvial excavation of sediment in valleys. The development of channelized flow in gullies also causes runoff to be more efficiently routed from the drainage basin, however, thereby decreasing infiltration and further increasing runoff in a positive feedback. This feedback suggests that once gully initiation is triggered by a shift in the balance between the colluvial infilling and fluvial excavation of sediment to/from valleys, it is very difficult to stop or reverse gully formation.

## CONCLUSIONS

The Tibetan Plateau has likely experienced many cycles of strengthened and weakened monsoon over the Quaternary similar to what it experienced during the last 20 k.y. Some of this cyclicality may be driving the regular alternation of deposition and pedogenesis visible in the foot-slope deposits as exemplified in Lhasa 6 (Fig. 4C). In any event, the hillslope deposits now exposed in gullies were extremely stable features for much of the Quaternary, gradually accumulating colluvial, eolian, and alluvial

sediments over many climate change cycles. Yet over this long time period, there is no stratigraphic evidence of deep incision into the deposits. The present deep (commonly 5–10 m), Holocene-age incision appears to be unprecedented. This raises the question: What is so unique about the Holocene?

Evidence suggests that anthropogenic deforestation was primarily responsible for the widespread mid-to-late Holocene gullying in drainage basins adjacent to the upper Tsangpo Valley. This hypothesis is consistent with the fact that, although the landscape was deforested multiple times during Pleistocene glacial intervals, the drier conditions that accompanied colder temperatures during glacial episodes apparently prevented gully development. Anthropogenic overharvesting/overgrazing, on the other hand, has occurred during the relatively wet climate of the mid-to-late Holocene and hence was more conducive to gully formation. Other recent studies make a strong case for human involvement in landscape degradation during the Holocene around Lhasa (Kaiser et al., 2006, 2009; Mieke et al., 2006, 2009). These studies have demonstrated that extensive erosion and colluviation in several drainages near Lhasa are mid-to-late Holocene in age. The results of this paper suggest that the deforestation that has occurred near Lhasa has likely occurred throughout the upper Tsangpo Valley.

## ACKNOWLEDGMENTS

We gratefully acknowledge the help of Lin Ding and his student Cai Fulong at the Institute of Tibetan Plateau Research at the Chinese Academy of Sciences in Beijing. Support for this project comes from U.S. National Science Foundation grants EAR-0438115 (to Quade) and HSD-0527620 (to Aldenderfer and Pelletier). We thank Oliver Korup and an anonymous reviewer for detailed reviews and constructive comments that helped improve the paper.

## REFERENCES CITED

- Adamiec, G., and Aitken, M.J., 1998, Dose-rate conversion factors: Update: *Ancient TL*, v. 16, p. 37–50.
- Aitken, M.J., 1998, *Introduction to Optical Dating*: Oxford, UK, Oxford University Press, 267 p.
- Aldenderfer, M.S., 2007, Modeling the Neolithic on the Tibetan Plateau, in Madsen, D.B., Chen, F.-H., and Gao, X., eds., *Late Quaternary Climate Change and Human Adaptation in Arid China: Developments in Quaternary Science*, v. 9, p. 151–162.
- Aldenderfer, M., and Zhang, Y., 2004, The prehistory of the Tibetan Plateau to the 7th C. AD: Perspectives and research from China and the West since 1950: *Journal of World Prehistory*, v. 18, p. 1–55, doi: 10.1023/B:JOWO.0000038657.79035.9e.
- Antevs, E., 1952, Arroyo-cutting and filling: *The Journal of Geology*, v. 60, p. 375–385, doi: 10.1086/625985.
- Bailey, R.M., and Arnold, L.J., 2006, Statistical modeling of single grain quartz  $D_c$  distributions and an assessment of procedures for estimating burial dose: *Quaternary Science Reviews*, v. 25, p. 2475–2502, doi: 10.1016/j.quascirev.2005.09.012.
- Betancourt, J.L., 1990, *Tucson's Santa Cruz River and the Arroyo Legacy* [Unpublished Ph.D. dissertation]: Tucson, Arizona, University of Arizona Press.

- Brantingham, P.J., Xing, G., Olsen, J.W., Haizhou, M., Rhode, D., Haiying, Z., and Madsen, D.B., 2007, A short chronology for the peopling of the Tibetan Plateau: Developments in Quaternary Sciences, v. 9, p. 129–150, doi: 10.1016/S1571-0866(07)09010-0.
- Burkard, M., and Kostaschuk, R.A., 1995, Initiation and evolution of gullies along the shoreline of Lake Huron: *Geomorphology*, v. 14, p. 211–219, doi: 10.1016/0169-555X(95)00059-E.
- Chang, D.H.S., 1981, The vegetation zonation of the Tibetan Plateau: *Mountain Research and Development*, v. 1, p. 29–48, doi: 10.2307/3672945.
- Collins, D.B.G., Bras, R.L., and Tucker, G.E., 2004, Modeling the effects of vegetation-erosion coupling on landscape evolution: *Journal of Geophysical Research*, v. 109, p. F03004, doi: 10.1029/2003JF000028.
- Cooke, R.U., and Reeves, R.W., 1976, *Arroyos and Environmental Change in the American Southwest*: Oxford, UK, Clarendon Press, 213 p.
- Culling, W.E.H., 1960, Analytical theory of erosion: *The Journal of Geology*, v. 68, p. 336–344, doi: 10.1086/626663.
- Culling, W.E.H., 1963, Soil creep and the development of hillslope slopes: *The Journal of Geology*, v. 71, p. 127–161, doi: 10.1086/626891.
- Ekern, P.C., 1951, Raindrop impact as the force initiating soil erosion: *Proceedings of the Soil Science Society of America*, v. 15, p. 7–10, doi: 10.2136/sssaj1951.036159950015000C0002x.
- Farnsworth, K.L., and Milliman, J.D., 2003, Effects of climatic and anthropogenic change on small mountainous rivers: The Salinas River example: *Global and Planetary Change*, v. 39, p. 53–64, doi: 10.1016/S0921-8181(03)00017-1.
- Gabet, E.J., and Dunne, T., 2003, Sediment detachment by rain power: *Water Resources Research*, v. 39, doi: 10.1029/2001WR000656.
- Galang, M.A., Markewicz, D., Morris, L.A., and Bussell, P., 2007, Land use change and gully erosion in the Piedmont region of South Carolina: *Journal of Soil and Water Conservation*, v. 62, p. 122–129.
- Galbraith, R.F., Roberts, R.G., Laslett, G.M., Yoshida, H., and Olley, J.M., 1999, Optical dating of single and multiple grains of quartz from Jinnium Rock Shelter, northern Australia: Part 1. Experimental design and statistical models: *Archaeometry*, v. 41, p. 339–364, doi: 10.1111/j.1475-4754.1999.tb00987.x.
- García-Ruiz, J.M., White, S.M., Lasanta, T., Martí, C., Gonzalez, C., Errea, M.P., and Valero, B., 1997, Assessing the effects of land-use changes on sediment yield and channel dynamics in the central Spanish Pyrenees, in Walling, D.E., and Probst, J.L., eds., *Human Impact on Erosion and Sedimentation*: Wallingford, UK, International Association of Hydrological Sciences, p. 151–158.
- Gomez, B., Banbury, K., Marden, M., Trustrum, N.A., Peacock, D.H., and Hoskin, P.J., 2003, Gully erosion and sediment production: Te Weraroa Stream, New Zealand: *Water Resources Research*, v. 39, no. 7, p. 1187, doi: 10.1029/2002WR001342.
- Goodrich, D.C., Lane, L.J., Shillito, R.M., and Miller, S.N., 1997, Linearity of basin response as a function of scale in a semiarid watershed: *Water Resources Research*, v. 33, no. 12, p. 2951–2965, doi: 10.1029/97WR01422.
- Graf, W.L., 1979, The development of montane arroyos and gullies: *Earth Surface Processes and Landforms*, v. 4, p. 1–14.
- Hack, J.T., 1957, *Studies of Longitudinal Stream Profiles in Virginia and Maryland*: U.S. Geological Survey Professional Paper 294-B, p. 45–97.
- Hall, S.A., 1977, Late Quaternary sedimentation and paleoecologic history of Chaco Canyon, New Mexico: *Geological Society of America Bulletin*, v. 88, p. 1593–1618, doi: 10.1130/0016-7606(1977)88<1593:LQSAHP>2.0.CO;2.
- Hanks, T.C., 2000, The age of scarplike landforms from diffusion-equation analysis, in Noller, J.S., Sowers, J.M., and Lettis, W.R., eds., *Quaternary Geochronology: Methods and Applications*: Washington, D.C., American Geophysical Union, p. 313–338.
- Harvey, A.M., 1992, Process interactions, temporal scales and the development of hillslope gully systems: Howgill Fells, northwest England: *Geomorphology*, v. 5, p. 323–344, doi: 10.1016/0169-555X(92)90012-D.
- Harvey, M.D., Watson, C.C., and Schumm, S.A., 1985, *Gully Erosion*: U.S. Department of the Interior, Bureau of Land Management Technical Note 366, 181 p.
- Herzschuh, U., Birks, H.J.B., Ni, J., Zhao, Y., Liu, H., Liu, X., and Grosse, G., 2010, Holocene land-cover changes on the Tibetan Plateau: The Holocene, v. 20, p. 91–104, doi: 10.1177/0959683609348882.
- Howard, A.D., 1994, A detachment-limited model of drainage basin evolution: *Water Resources Research*, v. 30, p. 2261–2286, doi: 10.1029/94WR00757.
- Howard, A.D., and Kerby, G., 1983, Channel changes in badlands: *Geological Society of America Bulletin*, v. 94, p. 739–752, doi: 10.1130/0016-7606(1983)94<739:CCIB>2.0.CO;2.
- Huang, X.Z., Chen, F.H., Fan, Y.X., and Yang, M.L., 2009, Dry late-glacial and early Holocene climate in arid central Asia indicated by lithological and palynological evidence from Bosten Lake, China: *Quaternary International*, v. 194, p. 19–27, doi: 10.1016/j.quaint.2007.10.002.
- Hughes, M.W., Almond, P.C., and Roering, J.J., 2009, Increased sediment transport via bioturbation at the last glacial-interglacial transition: *Geology*, v. 37, p. 919–922.
- Ijjasz-Vasquez, E.J., and Bras, R.L., 1995, Scaling regimes of local slope versus contributing area in digital elevation models: *Geomorphology*, v. 12, p. 299–311, doi: 10.1016/0169-555X(95)00012-T.
- Institute of Archaeology, Chinese Academy of Social Science and Bureau of Cultural Relics, Tibet Autonomous Region, 1999, *Qugong in Lhasa: Excavations of an Ancient Site and Tombs*: Beijing, Encyclopedia of China Publishing House.
- Institute of Geography, 1999, *National Physical Atlas of China*: Beijing, Chinese Cartographic Publishing House, 230 p.
- Istanbulluoglu, E., and Bras, R.L., 2005, Vegetation-modulated landscape evolution: Effects of vegetation on landscape processes, drainage density, and topography: *Journal of Geophysical Research*, v. 110, p. F02012, doi: 10.1029/2004JF000249.
- Istanbulluoglu, E., Tarboton, D.G., Pack, R.T., and Luce, C., 2003, A sediment transport model for incision of gullies on steep topography: *Water Resources Research*, v. 38, doi: 10.1029/2002WR001467.
- Istanbulluoglu, E., Tarboton, D.G., Pack, R.T., and Luce, C.H., 2004, Modeling of the interactions between forest vegetation, disturbances and sediment yields: *Journal of Geophysical Research*, v. 109, p. F01009, doi: 10.1029/2003JF000041.
- Kaiser, K., Mieke, G., Schoch, W.H., Zander, A., and Schultz, F., 2006, Relief, soil and lost forest: Late Holocene environmental changes in southern Tibet under human impact: *Zeitschrift für Geomorphologie Supplementband*, v. 142, p. 149–173.
- Kaiser, K., Ogenoorh, L., Schoch, W.H., and Mieke, G., 2009, Charcoal and fossil wood from palaeosols, sediments and artificial structures indicating late Holocene woodland decline in southern Tibet (China): *Quaternary Science Reviews*, v. 28, p. 1539–1554, doi: 10.1016/j.quascirev.2009.02.016.
- Li, X., Cheng, G., and Lu, L., 2005, Spatial analysis of air temperature in the Qinghai-Tibet Plateau: Arctic, Antarctic, and Alpine Research, v. 37, p. 246–252, doi: 10.1657/1523-0430(2005)037[0246:SAOATI]2.0.CO;2.
- Machette, M.N., 1985, Calcic soils of the southwestern United States, in Weide, D.L., and Faber, M.L., eds., *Soils and Quaternary Geology of the Southwestern United States*: Geological Society of America Special Paper 203, p. 1–21.
- Marden, M., Arnold, G., Gomez, B., and Rowan, D., 2005, Pre- and post-reforestation gully development in Mangatu Forest, east coast, North Island, New Zealand: *River Research and Applications*, v. 21, p. 757–771, doi: 10.1002/rra.882.
- Mieke, G., Mieke, S., Schultz, F., Kaiser, K., and Duo, L., 2006, Palaeoecological and experimental evidence of former forests and woodlands in treeless desert pastures of southern Tibet (Lhasa), A.R. Xizang, China: *Palaeogeography, Palaeoclimatology, Palaeoecology*, v. 242, no. 1–2, p. 54–67, doi: 10.1016/j.palaeo.2006.05.010.
- Mieke, G., Mieke, S., Schultz, F., Kaiser, K., and Duo, L., 2009, How old is pastoralism in Tibet? An ecological approach to the making of a Tibetan landscape: *Palaeogeography, Palaeoclimatology, Palaeoecology*, v. 276, no. 1–4, p. 130–147, doi: 10.1016/j.palaeo.2009.03.005.
- Moglen, G.E., and Bras, R.L., 1995a, The effect of spatial heterogeneities on geomorphic expression in a model of basin evolution: *Water Resources Research*, v. 31, p. 2613–2623, doi: 10.1029/95WR02036.
- Moglen, G.E., and Bras, R.L., 1995b, The importance of spatially heterogeneous erosivity and the cumulative area distribution within a basin evolution model: *Geomorphology*, v. 12, p. 173–185, doi: 10.1016/0169-555X(95)00003-N.
- Murray, A.S., and Wintle, A.G., 2000, Luminescence dating of quartz using an improved single-aliquot regenerative-dose protocol: *Radiation Measurements*, v. 32, p. 267–273, doi: 10.1016/S1350-4487(99)00253-X.
- Murray, A.S., and Wintle, A.G., 2003, The single-aliquot regenerative-dose protocol: Potential for improvements in reliability: *Radiation Measurements*, v. 37, p. 377–381, doi: 10.1016/S1350-4487(03)00053-2.
- Perron, J.T., Dietrich, W.E., and Kirchner, J.W., 2008, Controls on the spacing of first-order valleys: *Journal of Geophysical Research*, v. 113, p. F04016, doi: 10.1029/2007JF000977.
- Perron, J.T., Kirchner, J.W., and Dietrich, W.E., 2009, Formation of evenly-spaced ridges and valleys: *Nature*, v. 460, p. 502–505, doi: 10.1038/nature08174.
- Prescott, J.R., and Hutton, J.T., 1994, Cosmic-ray contributions to dose rates for luminescence and ESR dating: Large depths and long-term variations: *Radiation Measurements*, v. 23, p. 497–500, doi: 10.1016/1350-4487(94)90086-8.
- Prosser, I.P., and Dietrich, W.E., 1995, Field experiments on erosion by overland flow and their implication for a digital terrain model of channel initiation: *Water Resources Research*, v. 31, no. 11, p. 2867–2876, doi: 10.1029/95WR02218.
- Prosser, I.P., and Slade, C.J., 1994, Gully formation and the role of valley-floor vegetation, southeastern Australia: *Geology*, v. 22, p. 1127–1130, doi: 10.1130/0091-7613(1994)022<1127:GFATRO>2.3.CO;2.
- Prosser, I.P., and Soufi, M., 1998, Controls on gully formation following forest clearing in a humid temperate environment: *Water Resources Research*, v. 34, p. 3661–3671, doi: 10.1029/98WR02513.
- Rinaldo, A., Dietrich, W.E., Rigon, R., Vogel, G.K., and Rodriguez-Iturbe, I., 1995, Geomorphological signatures of varying climate: *Nature*, v. 374, p. 632–635, doi: 10.1038/374632a0.
- Roering, J.J., Kirchner, J.W., and Dietrich, W.E., 1999, Evidence for nonlinear, diffusive sediment transport on hillslopes and implications for landscape morphology: *Water Resources Research*, v. 35, no. 3, p. 853–870, doi: 10.1029/1998WR000090.
- Roering, J.J., Almond, P., Tonkin, P., and McKean, J., 2004, Constraining climatic controls on hillslope dynamics using a coupled model for the transport of soil and tracers: Application to loess-mantled hillslopes, Charwell River, South Island, New Zealand: *Journal of Geophysical Research*, v. 109, p. F01010, doi: 10.1029/2003JF000034.
- Rohrmann, A., Kapp, P., and Reiners, P., 2008, Minimal erosion in central Tibet since the Eocene and implications for plateau development: *Eos (Transactions of the American Geophysical Union)*, v. 89, abstract no. T32A–08.
- Rose, C.W., 1960, Soil detachment caused by rainfall: *Soil Science*, v. 89, p. 28–35, doi: 10.1097/00010694-196001000-00005.
- Simpson, G., and Schlunegger, F., 2003, Topographic evolution and morphology of surfaces evolving in response to coupled fluvial and hillslope sediment transport: *Journal of Geophysical Research*, v. 108, no. 2300, doi: 10.1029/2002JB002162.
- Smith, T.R., and Bretherton, F.P., 1972, Stability and the conservation of mass in drainage basin evolution: *Water Resources Research*, v. 8, p. 1506–1529, doi: 10.1029/WR008i006p01506.
- Soil Survey Staff, 1975, *Soil Taxonomy. A Basic System of Soil Classification for Making and Interpreting Soil*

- Surveys: U.S. Department of Agriculture Soil Conservation Service, *Agricultural Handbook*, Volume 436: Washington, D.C., U.S. Government Printing Office, 754 p.
- Sun, J., Li, S.-H., Muhs, D.R., and Li, B., 2007, Loess sedimentation in Tibet: Provenance, processes, and link with Quaternary glaciations: *Quaternary Science Reviews*, v. 26, p. 2265–2280, doi: 10.1016/j.quascirev.2007.05.003.
- Tarboton, D.G., 1997, A new method for the determination of flow directions and upslope areas in grid digital elevation models: *Water Resources Research*, v. 33, no. 2, p. 309–319, doi: 10.1029/96WR03137.
- Tarboton, D.G., Bras, R.L., and Rodriguez-Iturbe, I., 1992, A physical basis for drainage density: *Geomorphology*, v. 5, p. 59–76, doi: 10.1016/0169-555X(92)90058-V.
- Tucker, G.E., and Bras, R.L., 1998, Hillslope processes, drainage density, and landscape morphology: *Water Resources Research*, v. 34, p. 2751–2764, doi: 10.1029/98WR01474.
- Tucker, G.E., Arnold, L., Bras, R.L., Flores, H., Istanbuluoglu, E., and Solyom, P., 2006, Headwater channel dynamics in semiarid rangelands, Colorado high plains, USA: *Geological Society of America Bulletin*, v. 118, no. 7, p. 959–974, doi: 10.1130/B25928.1.
- Valentin, C., Poesen, J., and Li, Y., 2005, Gully erosion: Impacts, factors and control: *Catena*, v. 63, p. 132–153, doi: 10.1016/j.catena.2005.06.001.
- Walther, S.C., Roering, J.J., Almond, P.C., and Hughes, M.W., 2009, Long-term biogenic soil mixing and transport in a hilly, loess-mantled landscape: Blue Mountains of southeastern Washington: *Catena*, v. 79, p. 170–178, doi: 10.1016/j.catena.2009.08.003.
- Wang, Y.J., Cheng, H., Edwards, R.L., An, Z.S., Wu, J.Y., Shen, C.C., and Dorale, J.A., 2001, A high-resolution absolute-dated late Pleistocene monsoon record from Hulu Cave, China: *Science*, v. 294, p. 2345–2348, doi: 10.1126/science.1064618.
- Waters, M.W., and Haynes, C.V., 2001, Late-Quaternary arroyo formation and climate change in the American Southwest: *Geology*, v. 29, p. 399–402, doi: 10.1130/0091-7613(2001)029<0399:LQAFAC>2.0.CO;2.
- Webster, G.L., 1961, The altitudinal limits of vascular plants: *Ecology*, v. 42, p. 587–590, doi: 10.2307/1932249.
- Wells, N.A., and Andriamihaja, B., 1993, The initiation and growth of gullies in Madagascar: Are humans to blame?: *Geomorphology*, v. 8, p. 1–46, doi: 10.1016/0169-555X(93)90002-J.
- Whipple, K.X., 2004, Bedrock rivers and the geomorphology of active orogens: *Annual Review of Earth and Planetary Sciences*, v. 32, p. 151–185, doi: 10.1146/annurev.earth.32.101802.120356.
- Willgoose, G., 2005, Mathematical modeling of whole landscape evolution: *Annual Review of Earth and Planetary Sciences*, v. 33, p. 443–459, doi: 10.1146/annurev.earth.33.092203.122610.
- Willgoose, G., Bras, R.L., and Rodriguez-Iturbe, I., 1991, A coupled channel network growth and hillslope evolution model 1: Theory: *Water Resources Research*, v. 27, p. 1671–1684, doi: 10.1029/91WR00935.
- Zheng, Z., Yuan, B., and Petit-Maire, N., 1998, Paleoenvironments in China during the Last Glacial Maximum and the Holocene optimum: *Episodes*, v. 21, p. 152–158.

SCIENCE EDITOR: NANCY RIGGS  
ASSOCIATE EDITOR: JOAN FLORSHEIM

MANUSCRIPT RECEIVED 5 FEBRUARY 2010  
REVISED MANUSCRIPT RECEIVED 5 OCTOBER 2010  
MANUSCRIPT ACCEPTED 13 OCTOBER 2010

Printed in the USA